


REVIEW

Open Access



A Review of Smart Materials for the Boost of Soft Actuators, Soft Sensors, and Robotics Applications

Yufei Hao¹, Shixin Zhang², Bin Fang^{3*} , Fuchun Sun³, Huaping Liu³ and Haiyuan Li⁴

Abstract

With the advance of smart material science, robotics is evolving from rigid robots to soft robots. Compared to rigid robots, soft robots can safely interact with the environment, easily navigate in unstructured fields, and be minimized to operate in narrow spaces, owing to the new actuation and sensing technologies developed by the smart materials. In the review, different actuation and sensing technologies based on different smart materials are analyzed and summarized. According to the driving or feedback signals, actuators are categorized into electrically responsive actuators, thermally responsive actuators, magnetically responsive actuators, and photoresponsive actuators; sensors are categorized into resistive sensors, capacitive sensors, magnetic sensors, and optical waveguide sensors. After introducing the principle and several robotic prototypes of some typical materials in each category of the actuators and sensors. The advantages and disadvantages of the actuators and sensors are compared based on the categories, and their potential applications in robotics are also presented.

Keywords: Smart material, Soft robot, Actuator, Sensor

1 Introduction

During the decades, robots were mostly made of rigid components such as links and gears. The actuators (such as motors) and sensors (such as encoders) are installed in the joints [1]. By controlling the motion of motors via a program, robots can realize various locomotion [2]. Recently, the breakthrough in the research of smart materials opens a new direction for the research and development of soft robots [3]. Unlike stiff materials such as steel, smart materials are animate. They can be activated and respond to external stimuli such as electricity [4], heat [5], magnetism [6], and light [7]. Thus, their bodies can deform to generate motions such as bending [8], elongation [9], and torsion [10]. With these abilities, they

can be used as actuators to drive soft robots to achieve different kinds of locomotion.

To actively interact with the environments and control the kinematics and dynamics, sensors that can give feedbacks to different kinds of signals such as deformation and forces are indispensable for soft robots [11]. Because of the deformable characteristic of soft robots, sensors are required to be flexible or stretchable. To meet the requirements, many new flexible or stretchable sensors are developed. Based on the properties of materials, these sensors can convert the changing of deformation or force to the changing of the resistance [12], capacitance [13], magnetic field [14], or the intensity and reflection index of light [15].

In this review, we summarized the typical actuation and sensing technologies developed by smart materials. For actuation technologies, we categorized the actuators into electrically responsive actuators, thermally responsive actuators, magnetically responsive actuators, and photoresponsive actuators based on the driving signals. For

*Correspondence: fangbin@mail.tsinghua.edu.cn

³ Department of Computer Science and Technology, Tsinghua National Laboratory for Information Science and Technology, Tsinghua University, Beijing 100084, China

Full list of author information is available at the end of the article

each category, we introduced the principle and robotic prototypes of some representative materials. For sensing technologies, we classified them into four main types (resistive sensors, capacitive sensors, magnetic sensors, and optical waveguide sensors) based on the feedback signals. After introducing the details of each of the actuators and sensors, we compare their advantages and disadvantages and present potential robotic applications based on their characteristics.

2 Soft Actuators

2.1 Electrically Responsive Actuators

Electrically responsive materials can deform when they are exposed to an electric field, of which dielectric elastomers (DEs) are representative. DE is generally composed of two flexible electrode layers and a dielectric layer, where the dielectric layer is sandwiched between the electrode layers. Without activation, the dielectric layer does not deform. When a high voltage (generally the thousands of volts) is applied, the electric field between the two electrodes can generate Maxwell stress, which will squeeze the deformable dielectric layer, causing the decreasing thickness and the expansion of the area. This motion can convert electrical energy into mechanical energy.

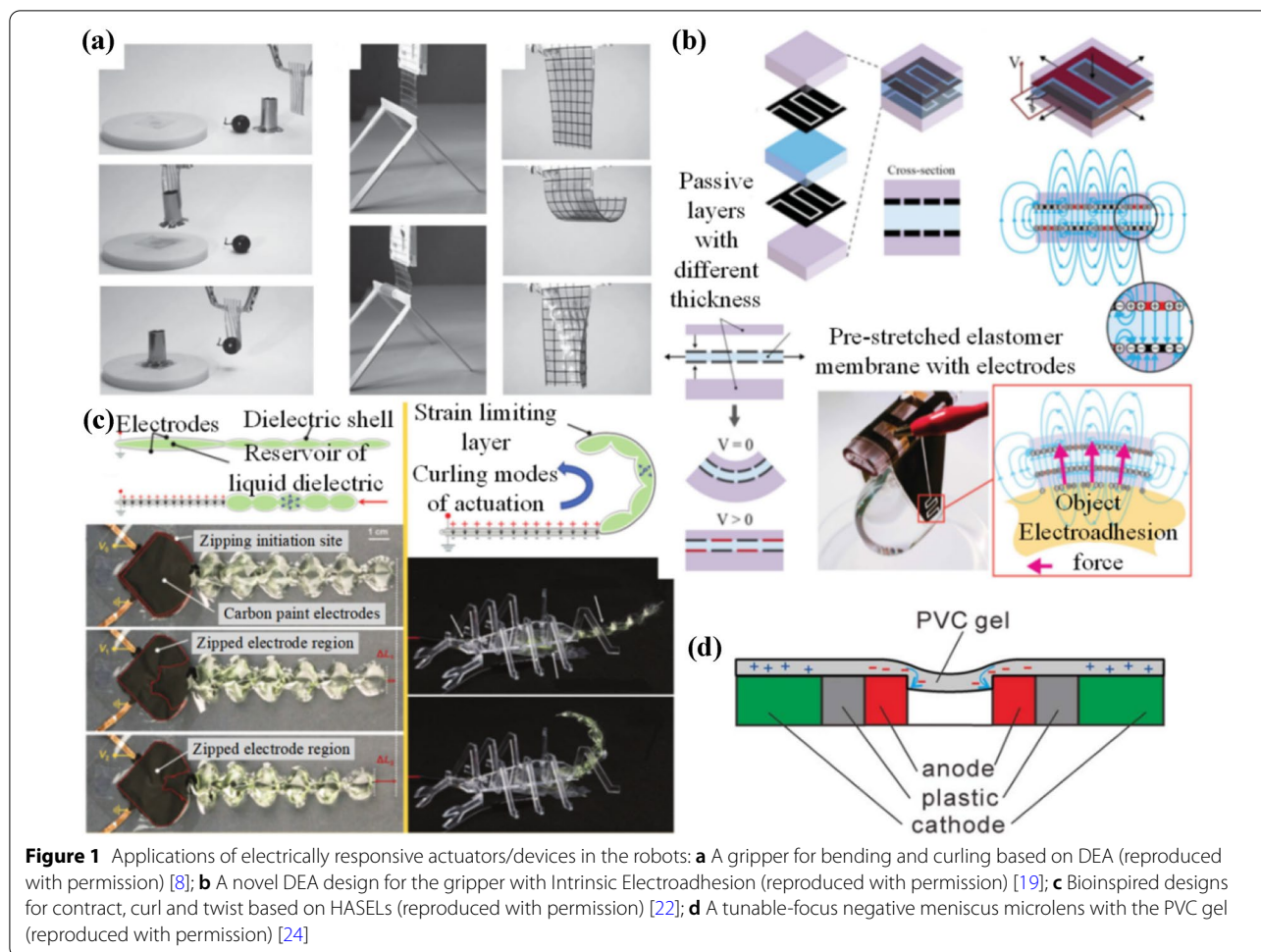
The electrostriction effect of the dielectric elastomer actuator (DEA) is widely used for actuation in soft robots. Compared with rigid actuators like motors, The structure of DEA is compact and many kinds of motion can be realized through a simple actuation methodology. For example, by fixing the edge of the circular DE and attaching a magnet on its surface, the DEA membrane can swell under high voltage, and recover to the initial shape by pulling the magnet when the voltage is off. This reciprocating motion can be used to make a microfluidic diaphragm pump [16]. By restricting the stretchability of one electrode layer, the entire DEA can be bent under the electric force, which is widely used in a variety of bionic robots. For example, using DEA as the legs and toes of a frog robot, the robot can swim if the DEA is periodically activated [4]. A similar method can be used to drive a robotic fish to swim [17]. By selectively controlling the deformation of DEA in different directions, more complex motions can be achieved. For example, using fiber to separately control the horizontal and vertical deformation, the DEA-based gripper can achieve various motions like bending and curling, which can be used to wrap and grasp objects (Figure 1(a)) [8]. To reduce the electric breakthrough of DEA, efforts have been taken to reduce the driving voltage by reducing the thickness of both the dielectric layer and the electrode layer. For example, the bioinspired insect robot [18] uses a double-layer carbon nanotube as the electrode layer, whose thickness is the

same as the molecular carbon nanotube. Besides, the thickness of the dielectric layer is only 6 μm , so the driving voltage can be reduced to only 450 V. Although the robot is only 190 mg in weight, it can carry a load of 950 mg, and move at a speed of 30 mm/s.

The high electric field can not only generate Maxwell stress to drive DEA but also generate electrical adhesion force (EA force), which is partly induced by the fringe electric field, for attaching. When separately applying high voltage and low voltage to two interdigitated electrodes, the adjacent electrodes can generate alternating positive and negative charges; this induces antipolar charges on the adjacent surface of the object. Thus, the EA force generates between the electrode and the objects, which can significantly increase the shear force than normal force. This EA force is extensively used for grasping and attaching in robotic applications. Figure 1(b) shows a special gripper based on DE and EA. The gripper is achieved by sandwiching a pre-stretched membrane and electrodes with two flexible layers with different thicknesses. When the voltage is off, the internal stress caused by the pre-stretched membrane and different thicknesses of the flexible layers makes the entire structure bend. When the voltage is on, the membrane extends under the Maxwell force, causing the entire structure to stretch and flatten. At the same time, the interdigitated electrodes at the bottom will generate EA force to attract the object [19]. EA force is also widely used in biomimetic climbing robots. For example, the robot [20] can use its EA foot to adhere to the surface and use DEA to move the EA foot, thus achieves the wall climbing function.

For the dielectric layer, recent researches begin to explore insulating liquid besides the solid elastomers, which lead to the generation of the HASEL actuator. The structure of the HASEL actuator is dielectric liquid sandwiched between two flexible electrodes. Under the high electric field, the electrodes can squeeze the liquid to the side under the Maxwell force. This new actuator can be also deployed in robots. By extruding the liquid from the middle to the side, the height of the entire actuator is increased, thus can generate force to grasp objects [21]. The linear contraction and bending can also be achieved by extruding the liquid from the storage area to flexible chambers with different geometric structures, as are shown in Figure 1(c) [22].

Besides DE, there exist other electrical response materials that can deform by transporting ions or dielectric particles under the electric field, such as the ionic polymer metal composites (IPMC), which are composed of an ionic polymer whose surfaces are coated with conductors. Under hydration, the positive ions in the polymer can move freely, while the negative ions are bonded with the carbon chains in the polymer. Under the electric



field, the positive ions tend to concentrate near the cathode, which causes a higher concentration of surrounding molecules and produces local stress to bend the structure. IPMC can only work in water, but it can generate higher strain under lower voltage. Therefore, it has promising applications in underwater robots, such as the biomimetic robot fish [10]. Polyvinyl chloride (PVC) is also an ion-driven smart material. These actuators usually consist of PVC gel sandwiched between solid or meshed electrodes. Under the electric field, the PVC gel can be polarized. The generated anions creep towards the anode, which generates force and deformation [23]. The peristaltic direction of anions can be controlled by the design of the structure and the position of the electrodes, thus generate different kinds of motion. As shown in Figure 1(d), by driving anions to move to the sidewall of the anode, the lens can change its focus [24]. What's more, Electrorheological fluid (ER fluid) is also an electric responsive material. It is usually a suspension liquid, with high dielectric constant particles suspended in low dielectric constant oils. Under normal conditions,

the viscosity of ER fluid is low. Under the electric field, the particles arrange in the direction of the electric field, reading to the increase of the viscosity. ER fluid is widely used in microfluidic valves [25].

2.2 Thermally Responsive Actuators

When the thermally responsive materials are heated to a certain temperature by directly joule heating or indirectly heating via ultraviolet waves, the molecular constitution of the materials can be changed, resulting in the decline of their elastic modulus or contraction deformation. Shape Memory Polymer (SMP), whose elastic modulus drops sharply when they are heated above the glass conversion temperature, is one of the thermally responsive materials. Its elastic modulus can be decreased by hundreds of magnitudes, thus it is widely used in variable stiffness robots [26]. SMP can also have the shape memory effect via a temperature program. First, stretch the SMP when the temperature exceeds the glass transition temperature. Then remove the tension when the SMP is cooled down, it can remain in the stretched state.

By heating, it can return to its original shape. This shape memory effect has been widely applied in self-folding or self-reconfiguration robots. By deploying SMP at the joints of the origami robots, the robots can automatically fold from 2D to 3D after heating [27]. SMP can also be programmed to unfold from a bending state, thus the reconfigurable mechanism can be driven to reconfigure from 2D to 3D [28]. By heating the SMP, the miniature gripper can also bend to wrap and grasp objects. As the elastic modulus of the gripper is increased after cooling, it can lock the objects without any additional energy consumption [29] (Figure 2(a)).

Although SMPs have advantages of variable stiffness and shape memory, after they are heated to the initial state, they cannot go back to the programmed state without external forces. By contrast, liquid crystal elastomers (LCE) can realize bidirectional deformation under temperature control. LCE is usually composed of mesogens embedded into the polymer chain. Mesogen is usually a polarized long strip molecule, which can easily change directions under the electric field. At the normal temperature, the mesogens of LCEs are well ordered. When heated, the mesogens are disordered, so the LCE turns to isotropic and contracts at the same time. When cooled, the mesogens return to their original sequence and the

shape of the LCE is recovered. The thermal induced contraction effect of LCE is widely used in soft microrobots. For example, by assembling the polyimide multi-layered structure, the entire structure can bend towards the polyimide film direction when it is heated to contract the LCE layer. By separately controlling the temperature of different locations of LCE, the local bending of the entire structure can be achieved, thus the robot can move like an inchworm [3] (Figure 2(b)). More complicated motion can also be achieved by limiting the contracting position of the LCE with structural design. As shown in Figure 2(c), by crosswise arranging higher stiffness silicone rubber on the upper and lower surface of LCE, the LCE cannot contract at these locations. Thus the structure can achieve caterpillar-like locomotion when it is heated through ultraviolet light [30]. In addition to LCE, PVC can also contract when heated. So it can be arranged at the joint to drive the self-folding robot [31].

Shape memory alloy (SMA) is also a thermally responsive material that can realize bidirectional deformation. When the temperature of SMA is below the phase transition temperature, it is in the martensite state and can deform under external forces. When the temperature is above the phase transition temperature, SMA is in the austenite state, the deformation at low temperature can

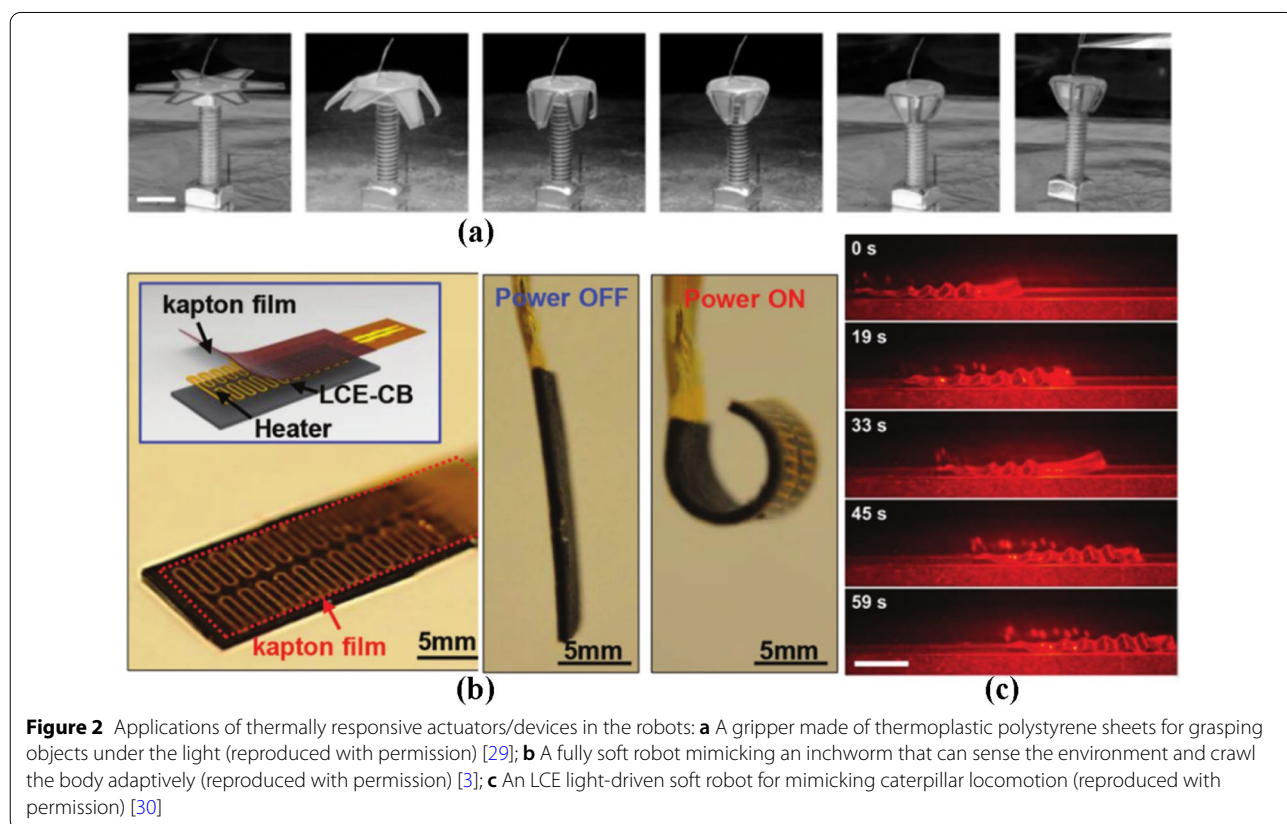


Figure 2 Applications of thermally responsive actuators/devices in the robots: **a** A gripper made of thermoplastic polystyrene sheets for grasping objects under the light (reproduced with permission) [29]; **b** A fully soft robot mimicking an inchworm that can sense the environment and crawl the body adaptively (reproduced with permission) [3]; **c** An LCE light-driven soft robot for mimicking caterpillar locomotion (reproduced with permission) [30]

be eliminated and the initial shape can be recovered. The shape memory effect of SMA is widely used in biomimetic robots. By distributing SMA coils along the circumferential and axial direction, the ‘Meshworm’ robot can squirm like worms. And it can still move after hit by the hammer [5]. The biomimetic octopus tentacles can also bend and curl by controlling the contraction of SMA coils along the circumference direction [9]. Besides, SMA coils can be attached to the back of the biomimetic caterpillar robot to drive it to curl and bounce [32].

2.3 Magnetically Responsive Actuators

Magnetically responsive materials are mostly composites that mix magnetic particles with soft materials such as silicone. Magnetic particles can be magnetized by the magnetic field to generate regular magnetization curves, whose direction and amplitude can be changed. Under the magnetic field, the magnetized particles interact with the spatially distributed magnetic field and turn to align with the spatial magnetic field. Thus, the torque can be produced to shrink, elongate, or bend the entire material. Because the magnetic field can penetrate a lot of mediums, magnetically responsive actuators are an ideal choice for the operation in confined space and are widely used in untethered microrobots. And different kinds of actuators can be developed by changing the driving signal, the magnetization curves, and the shape and stiffness of the material. As is shown in Figure 3, under the external oscillating magnetic

field, the micro jellyfish robot can drive the surrounding fluid to flow in different directions, so the robot can float upward and downward [6]. By controlling the magnetization curve direction via the magnetic field, the multimodal micro robot can locomote between different liquids and terrains by changing its modes, such as swimming inside or on the surface of the liquid, climbing a platform, rolling, or walking on the surface, bypassing the obstacles or crawling in narrow tunnels [33]. Furthermore, the magnetization and programming of the magnetic particles can be achieved via 3D printing. By fixing the magnetic or electromagnetic field around the printing nozzle, the ferromagnetic particles in the composite ink can be magnetized during printing, so they can arrange along the direction of the magnetic field. In this way, a variety of robots with complex magnetization curves can be printed, which can execute specific complex movements under the magnetic field [34]. The size of the printed continuum robot can be a submillimeter scale and the robot can move freely under the guidance of the magnetic field. Compared to the cable-driven or pneumatic continuum robots, the magnetically responsive robots are not only untethered but also more flexible, which is a promising direction for robots operating in narrow spaces [35]. One disadvantage of these kinds of actuators is that their movement is specifically designed and cannot change after fabrication. To overcome this, a new type of electromagnetic actuator, which usually contains

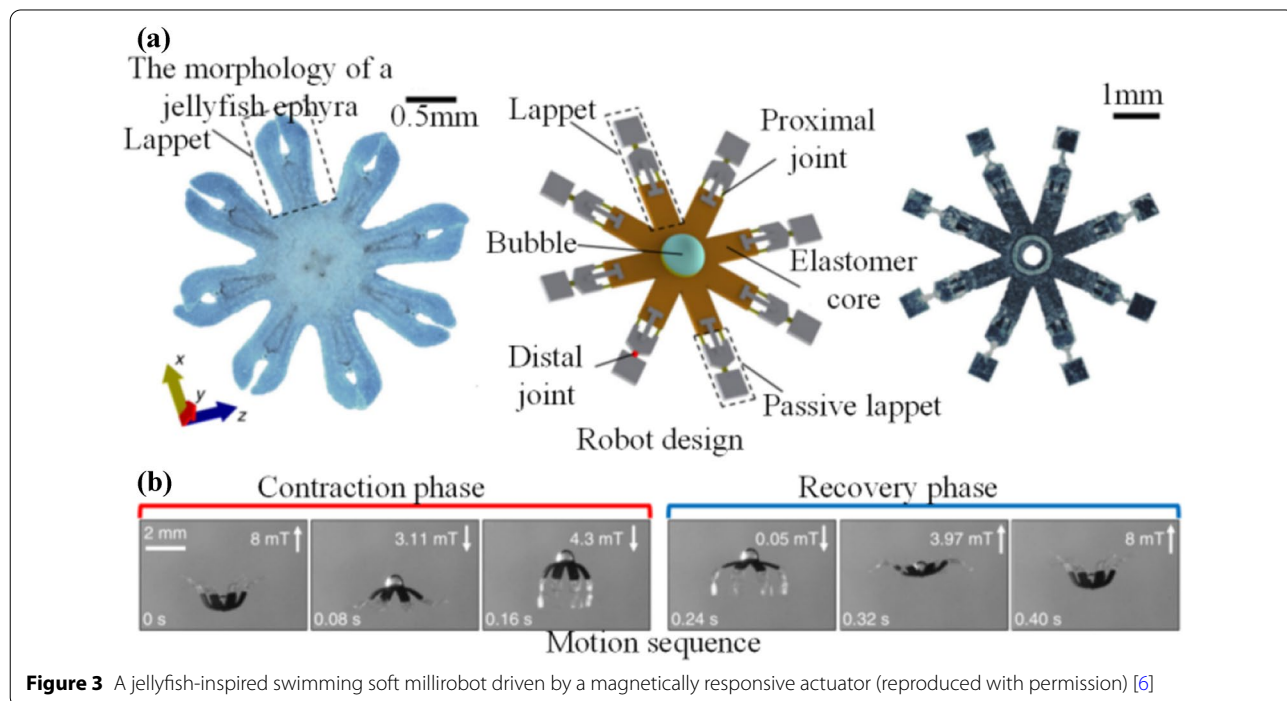


Figure 3 A jellyfish-inspired swimming soft millirobot driven by a magnetically responsive actuator (reproduced with permission) [6]

liquid metal or flexible coils and can be maneuverable by the Lorentz force, is developing [36].

2.4 Photoresponsive Actuators

Photoresponsive actuators are usually made by adding light-sensitive fillers to polymers such as silicone and liquid crystal elastomer. Under the light, they can bend, contract, or expand, and these deformations are reversible. By changing the wavelength, intensity, and irradiation time of light, these actuators can be programmed to have a specific response and achieve the desired motion. Light can also trigger photochemical reactions, which provide energy to drive the robot. The micromotor in Figure 4(a) uses Bismuth oxyiodide (BiOI) as a photocatalyst to trigger a series of oxidation and reduction reactions to drive the robot to move forward automatically. The micromotor consists of two hemispheres, one of which is covered with metal while the other is covered with BiOI. Under visible light, electrons in

BiOI are attracted to the metal side and gather here. While H⁺ ions produced by water oxidation gather on the BiOI hemisphere. To balance the negative charges on the metal hemisphere, H⁺ ions migrate from the BiOI hemisphere to the metal hemisphere, where reduction reactions occur with electrons. The migration of H⁺ ions is accompanied by the electroosmosis of water molecules to the metal hemisphere, which drives the micro-motor to move forward [37] (Figure 4(a)). By incorporating an azobenzene derivative Disperse Red 1 acrylate into the liquid crystal network (LCN), the water inside the mixture can be desorbed when heated by the light, and the material proceeds deswelling. Without light, the material absorbs water to swell again. With this principle, a bionic flower can automatically fold under light and unfold when the light is off [38] (Figure 4(b)). Similarly, the 3D-printed flower, which is made of SMP mixed with carbon black, can also be programmed to bloom under the light [39]

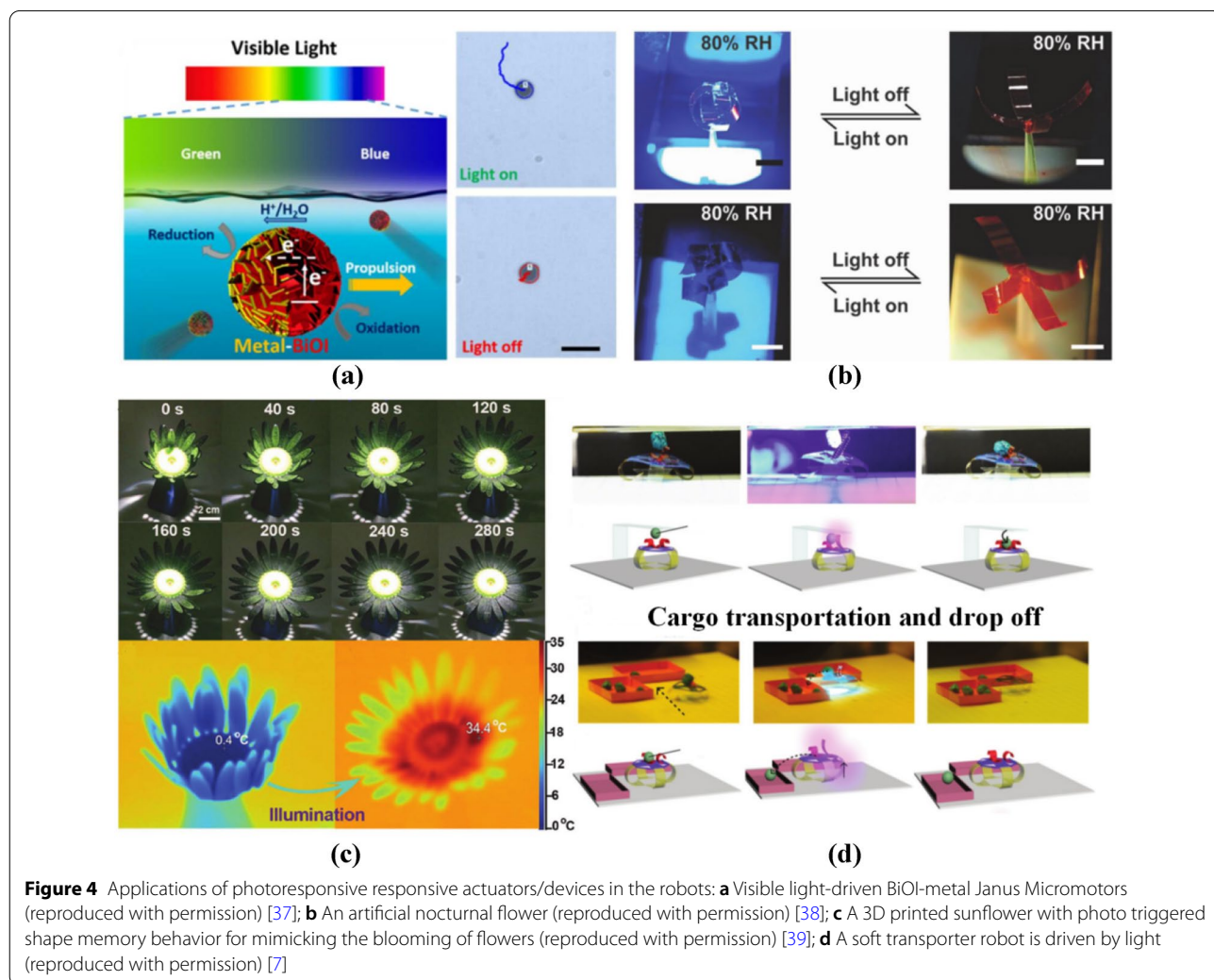


Figure 4 Applications of photoresponsive responsive actuators/devices in the robots: **a** Visible light-driven BiOI-metal Janus Micromotors (reproduced with permission) [37]; **b** An artificial nocturnal flower (reproduced with permission) [38]; **c** A 3D printed sunflower with photo triggered shape memory behavior for mimicking the blooming of flowers (reproduced with permission) [39]; **d** A soft transporter robot is driven by light (reproduced with permission) [7]

Table 1 Comparison and potential application of soft actuators in robotic

	Soft actuator				Electrically response actuator			Thermally responsive actuator			Magnetically responsive actuator	Photoresponsive soft actuator
	DE	Insulating liquid	IPMC	PVC	ER fluid	SMP	LCE	SMA	magnetic particles	Photoresponsive material		
Response time	< 200 μs	0.01–0.05 s	> 2 s	< 0.2 s	~10 ⁻³ s	10–40 s	> 60 s	0.2–2 s	< 1 s	1.8–9 s		
Advantages	High energy density; Fast response; Lightweight Low noise	Self-healing; Reliable	High flexibility; Low driving voltage; Large bending	Stable; Durable; Fast response;	Fully flexible	Variable stiffness	Compliant; Reversible deformation	High energy density	Small size; Non-invasiveness; High mobility; Untethered	Simple structure; Miniaturization; Lightweight; Untethered		
Limitations	Dielectric breakdown; High voltage	High voltage; Leakage	Low efficiency; Limited lifetime	Electrical breakdown	Compliant and robustness	Unidirectional deformation; Low efficiency	Limited efficiency	Uncertain fatigue behavior	Magnetic interference; Low efficiency	Low efficiency; Slow response		
Application	Biomimetic robots; Underwater robots; Grasping tasks, etc.	Biomimetic structures; Grasping tasks, etc.	Underwater robots, etc.	Micro electronics; Optical devices, etc.	Microfluidic diaphragm pumps, etc.	Self-folding and self-reconstructing robots, etc.	Micro-soft robot, etc.	Underwater robots, etc.	Micro Untethered robot; Submillimeter continuous robots, etc.	Micromotor; Simulation of the flower bloom, etc.		

(Figure 4(c)). By adding photothermal mono acrylate azobenzene derivatives, which absorb lights of specific wavelengths, into LCN, the material can release heat by isomerization and thermally expand under the light. Combing with mechanical design, the bent structure can be straightened under the light. As the micro-transfer robot shows in Figure 4(d), by controlling the bending of the legs and gripper of the robot, it can perform serials of tasks such as grasping, transporting, and delivering goods [7].

2.5 Potential Application in Robotics

In Table 1, driven by the electric field, electrically responsive materials have the characteristics of high energy density and fast response. However, DEAs have the disadvantages of electric breakthrough and safety issues due to the high voltage. Other electrically responsive actuators such as IPMC can be actuated under low voltage, but the output force is not big. Thermally responsive materials can not only be used to actuate robots but also to change their stiffness. However, the heating and cooling speed is a big issue. What's more, the stability and repeatability of these materials need further verification. Because of the high penetrability of the magnetic field, magnetically responsive actuators can achieve untethered locomotion in unstructured environments. Also, these actuators can be scaled down to smaller sizes to be deployed in narrow spaces. What's more, these actuators can achieve complicated motions compared to the other two actuators, but the requirement of the magnetic field is also strict. Like magnetically responsive actuators, photoresponsive actuators have advantages of miniaturization, simple structure, and teleoperation. However, the response speed is slow, and the efficiency also needs to improve.

For robotic applications (Table 1), electrically response actuators such as DEAs can be used to actuate robots under high frequencies, such as the flapping of bees, the jumping of insects, the swinging of fishes, and the vibrating of diaphragm pumps. If the driving voltage can be further decreased and the power source can be portable, these robots can be deployed in many scenarios, such as undersea sampling, post-disaster rescue, and military scout. With thermal programming, thermally responsive materials can achieve many functions like shape memory, one-directional or reversible deformation, and stiffness changing. Therefore, they can be deployed in variable stiffness robots to increase their load capacity, bioinspired robots to study the kinematics of animals, and self-reconfigurable robots for the changing of shapes and configurations. But, as we mentioned before, the response speed needs to be further improved. With the advantages of miniaturization and untethered actuation, magnetically responsive actuators are the ideal choice for

applications in unstructured, confined, and watery environments, such as targeted drug delivery, in vivo monitoring, and microsurgery. Photoresponsive actuators can also achieve untethered operations, as mentioned like the self-folding flower, micro motor, and the delivery robot. But related researches are still limited in the stage of the material study. With the maturing of related technologies, we believe these actuators can be deployed in some scenarios with no electricity but light source like sunlight.

3 Soft Sensors

3.1 Resistive Sensors

Resistive sensors can convert the change of external signal into the change of resistance. Based on the formula $R = \rho l/s$ (R is the resistance, ρ is the electric resistivity, l is the length, and s is the cross-sectional area), the resistance can change if l or s is changed. Therefore, the basic principle of resistive sensors is to convert the deformation or force information into the change of l or s , then change the resistance value.

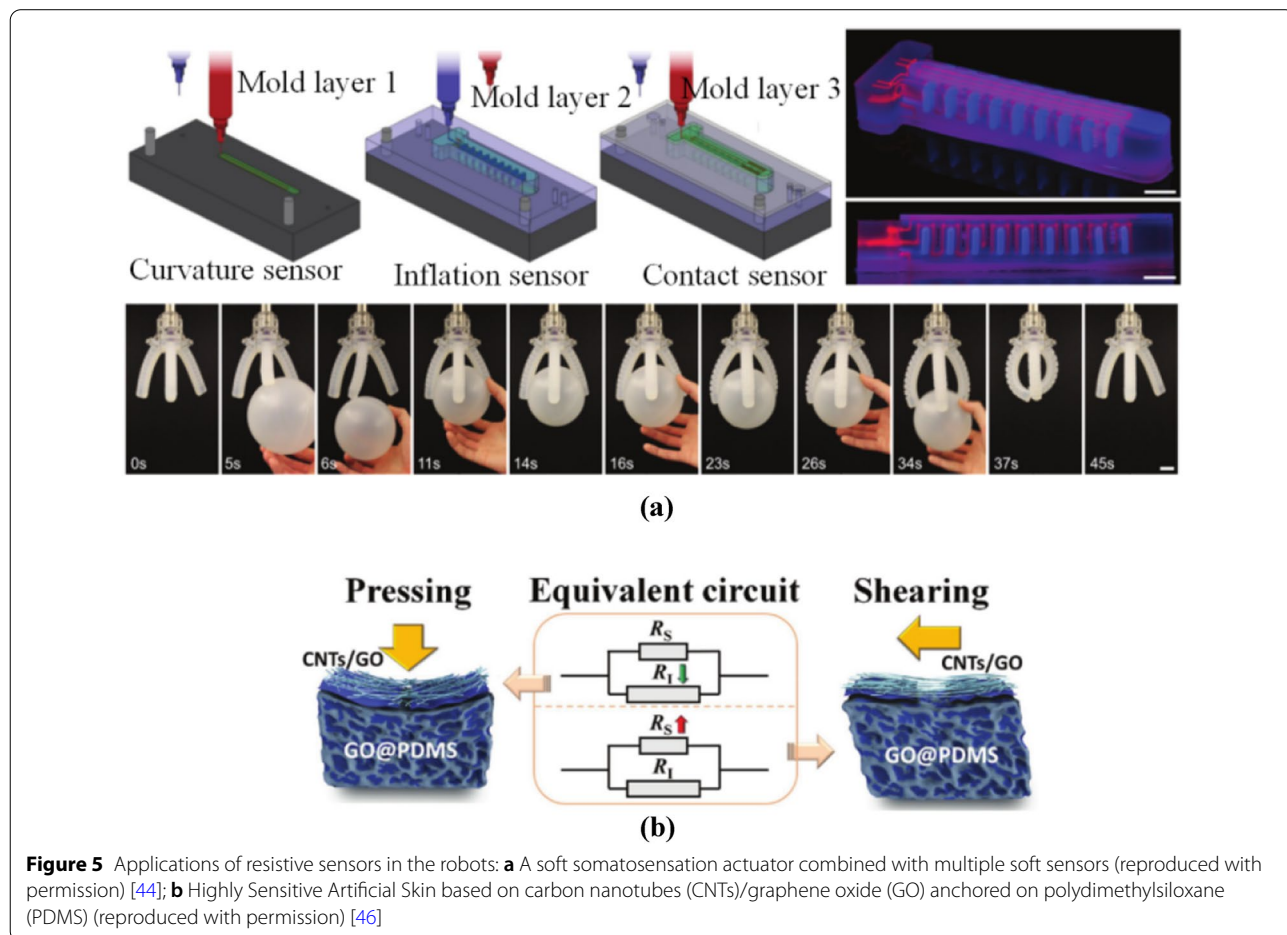
To measure different signals such as stretching, normal force, and shear force, resistive sensors are designed for different structures with different conductive materials. And the structures can deform under specific forces, thus the sensors can give feedbacks to those forces. Liquid metal, which is liquid at room temperature and has the ability of high conductivity and amorphism, is one of the various conductive materials and is widely used in various resistive sensors. When liquid metal is injected into microfluidic channels, the channels deform under external loads, and the resistance of liquid metal changes. This resistance change can be calibrated to measure the related loads. For example, the resistive sensor [12] is composed of three different channel layers. The channels in the bottom two layers are orthogonally zigzagged, and the resistances of the liquid metal inside these channels increase if the channels are separately stretched in X and Y direction. The channel in the upper layer is spiral, and the resistance of the liquid metal in the channel increases if the channel is compressed. The resistive sensor [40] has a rigid bump on top of the independent liquid metal channels. Under a specific force, the bump compresses the channel in that force direction, so the resistance of the liquid metal in that channel is changed and the sensor can measure the force in that direction. Similarly, the sensor [41] has four channels that are equally distributed in a circle underneath a semispherical bump. Under normal pressure, the resistances of the liquid metal in all the channels increase. Under shear force, the resistance of the liquid metal in one channel decreases while that in the opposite channel increases, so the sensor can measure not only the amplitude of the shear force but also its direction.

Besides liquid metal, other conductive materials can also be used in resistive sensors. For example, the wearable sensing glove [42] is made by injecting hydrogel mixed with lithium chloride into the silicone channels. Then the hydrogel can be solidified under ultraviolet light. As the fingers move, the hydrogel in the channels is stretched, its resistance increases. So, the bending angle of the fingers can be measured. By growing carbon nanotubes (CNTs) at the two sides of a micro silicone bump via MEMS fabrication, the sensor can measure the normal force and shear force based on the resistance change of the two sides [43]. By making ionic conductive gel into ink, it can be directly printed inside the 3D structure of the silicone rubber finger to deploy three different sensors: curvature sensor, air pressure sensor, and force pressure sensor [44] (Figure 5(a)). This 3D printing method opens a new way for the fabrication of sensing and actuation integrated robots. Furthermore, the resistance can also be changed with a special structure design. By laser cutting the conductive silicone rubber sheet into the kirigami structure, the resistance of the structure increases when it deforms greatly under a small

tension. By attaching the sensor to the surface of a continuum robotic arm, the spatial posture of the arm can be calculated with the assistance of the feedback of the sensors [45]. In Figure 5(b), the resistive sensor is achieved by the micropore structure of the graphene oxide (GO) [46]. The sensor is composed of two layers, one of which is the composite of CNTs and GO while the other is a composite of GO and PDMS. Under normal pressure, the micropores in the lower layer are squeezed so the GO aggregates and the resistance decreases. Under shear force, the CNTs in the upper layer are stretched and the resistance increases. The micro hair-based sensor is realized by the overlapping and interlocking of two platinum-coated PDMS fiber structures [47]. When subjected to different forces such as normal force, shear force, and torque, the interlocked micro hair structure can deform differently, so the sensor can measure these forces.

3.2 Capacitive Sensors

Capacitive sensors can convert external signals such as deformation and pressure into the change of capacitance. With different structural designs, capacitive sensors can



measure different signals. In robotic applications, the parallel plate capacitance sensors, which are generally a dielectric layer sandwiched between two electrode plates, are widely used. According to the formula of the parallel plate capacitance: $C = \epsilon_0 \epsilon_r s / d$ (C is the capacitance, ϵ_0 is the absolute dielectric constants, ϵ_r is the relative dielectric constants, s is the overlapping area between the two parallel plates, and d is the distance between parallel plates), When s or d is changed, the capacitance of the parallel plate is also changed. Therefore, the basic principle of the sensors is to convert the signal we are going to measure to the change of s or d , then the change of capacitance.

The simple parallel plate capacitance sensor can be utilized to measure the unidirectional strain and normal force. The sensor in Figure 6(a) is an example of the measurement of strain. By sandwiching the elastomer dielectric layer with two stretchable conductive fiber cloth, the thickness of the dielectric layer decreases, and the area increases under stretch, so the capacitance increases [13].

Under normal pressure, the distance between the two parallel electric plates decreases by pushing the elastomer dielectric layer, and the capacitance increases. Therefore, the sensor can measure normal pressure. Because the elastomer is incompressible, the sensitivity and accuracy of the sensor are low if we use a solid elastomer as the dielectric layer. To improve this, many capacitance sensors with microstructured dielectric layers are developed. Compared to the solid dielectric layer, the microstructured dielectric layer can not only decrease the gap between the two electric plates under the same pressure but also increase the equivalent dielectric constant when the pores are compacted. The pyramid structure, which can be fabricated via the etched silicon wafer, is one of the representative microstructures [48]. With a maximum size of 6 μm for the microstructure, the sensor can be very thin but with high sensitivity (Figure 6(b)). By plasma treating the top surface of the pre-stretched PDMS film, micro wavy structures can generate when the PDMS film is released [52] (Figure 6(d)). Because the

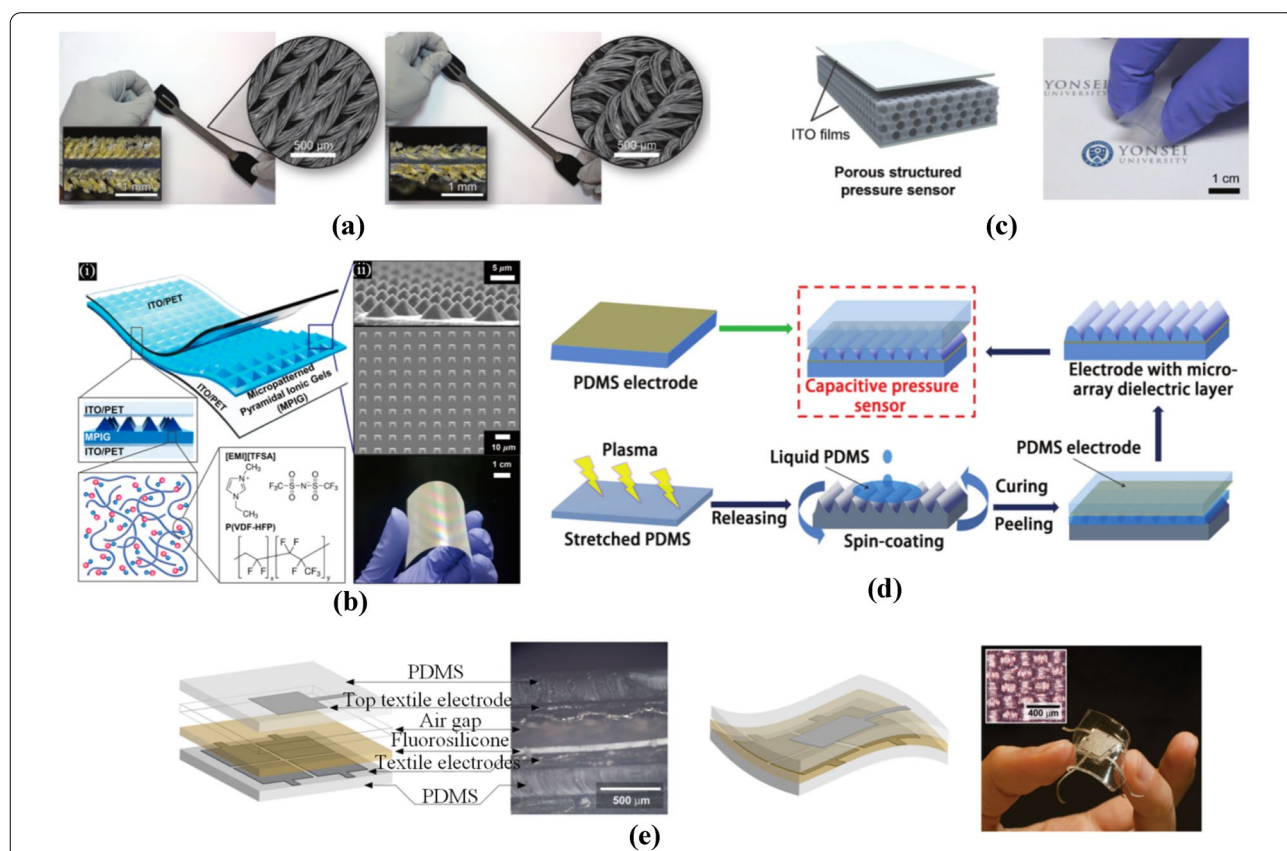


Figure 6 Applications of capacitive sensors in the robots: **a** Composite textile-silicone capacitive strain sensor (reproduced with permission) [13]; **b** A mechanically flexible capacitive type pressure sensor based on micropatterned pyramidal ionic gels (reproduced with permission) [48]; **c** A highly sensitive capacitive pressure sensor based on polydimethylsiloxane (PDMS) thin film (reproduced with permission) [49]; **d** A capacitive flexible pressure sensor based on the micro-arrayed PDMS dielectric layer (reproduced with permission) [52]; **e** A fully flexible capacitive three-axial force sensor made with conductive fabric electrodes and an elastomeric material (reproduced with permission) [54]

top surface of the PDMS film cannot recover to the initial state after plasma treatment. What's more, porous dielectric layers can also be fabricated by adding a porogen to the PDMS. As the sensor in Figure 6(c) shows, by mixing polystyrene beads with uncured PDMS, and dissolving the beads via dimethylformamide after the PDMS cured, a homogeneous porous dielectric layer can be fabricated [49]. Besides the polystyrene beads, other falsifiable or soluble materials, such as NH_4CO_3 , sugar, and salt, can also be used as porogen for the fabrication of a porous dielectric layer [50, 51].

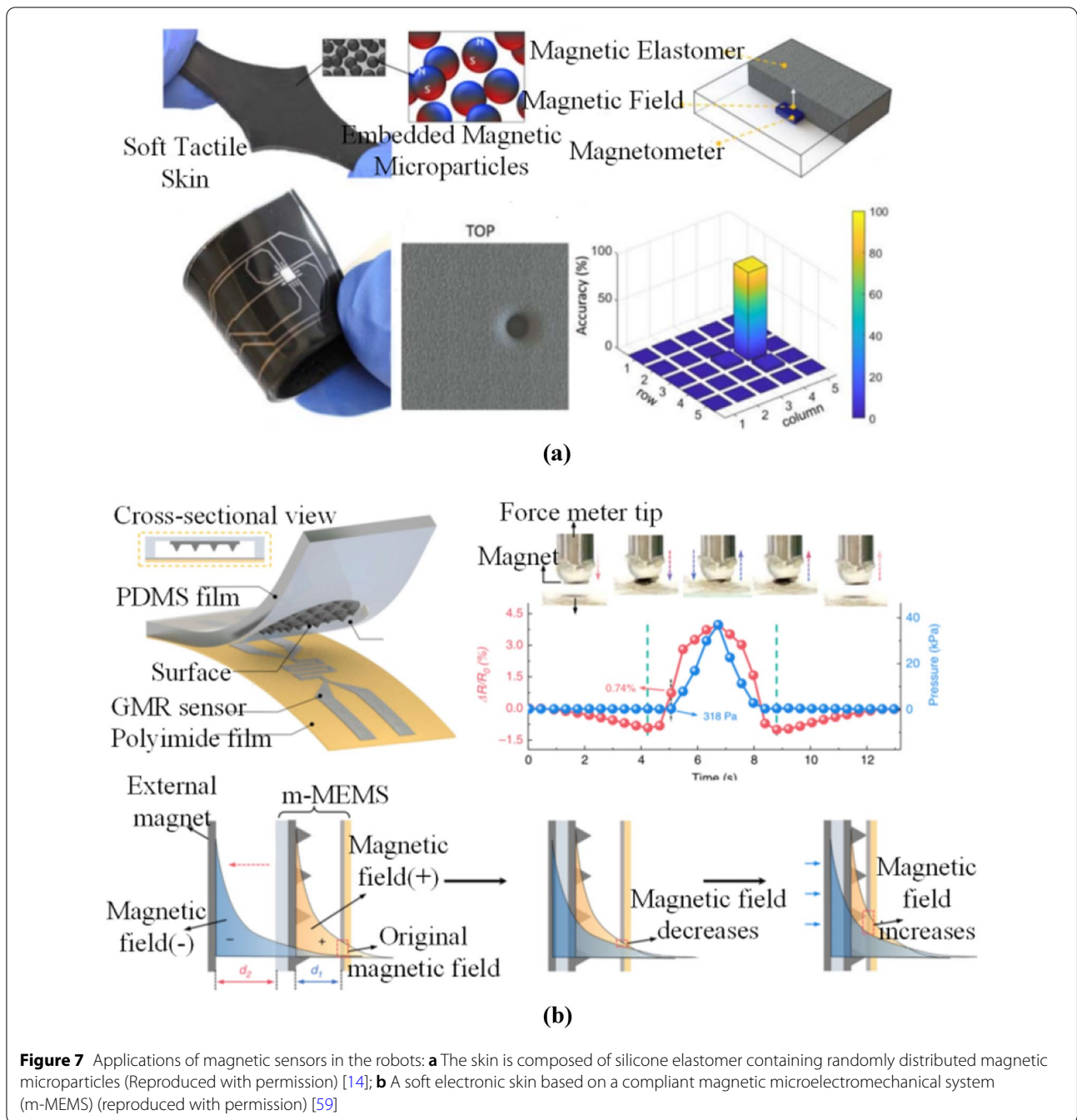
By increasing the number of electrodes and changing their relative positions, multi-dimensional forces can be measured utilizing the capacitance differences between different electrodes. As the capacitance sensor [53] shows, its 5 electrodes (E5 in the upper layer and E1–E4 in the lower layer equally arranged in a circular) constitute 4 capacitors. Under normal pressure, the capacitances of all the capacitors increases, thus the sensor can measure normal forces. Under shear pressure in the X direction, the capacitance between E2 and E5 increases/decreases, and the capacitance between E4 and E5 decreases/increases simultaneously, so the sensor can measure the magnitude and direction of shear force in the X -direction. In the same way, the sensor can also measure the magnitude and direction of the shear force in the Y direction. The capacitance sensor in Figure 6(e) has a similar principle but uses conductive fibers as the electrodes. The four electrodes in the lower layer arrange in a 2 by 2 matrix. Under shear pressure, the capacitance of the two capacitors in the same column increases/decreases, while the capacitance of the other two capacitors in the other column decreases/increases. Therefore, the sensitivity and resolution of the sensor can increase. The air cavity in the center can further increase the sensitivity [54]. The fringing effect of capacitance can also be used to measure forces in different directions. The capacitance sensor [55] is composed of three layers: bump layer, structural layer, and flexible printed circuit board (FPCB) layer. The structural layer is an air cavity. In the FPCB layer, fringing capacitances exist between the center electrode and the surrounding four electrodes. Under different normal and shear forces, the bump will cause different deformation in the structural layer, and change the distribution of electric fields between the central electrode and surrounding electrodes, further the change of capacitances. Ref. [56] shows a 3D force capacitance sensor which is inspired by the dermal-epidermal interface structure in human skin. The sensor is composed of a series of capacitors that distribute above and around the bump. Under normal or shear forces. The capacitance of each capacitor changes differently. Thus, the sensor can measure the magnitude, direction, and

angle of the force by taking advantage of the capacitance distribution. The pyramid microstructure in the upper layer can further increase the sensitivity and decrease the response time of the sensor.

3.3 Magnetic Sensors

Magnetic sensors, which usually consist of two components: magnetic parts and Hall sensors, can convert external information such as forces and deformation into the change of magnetic fields. The magnetic parts are usually permanent magnets or soft composited composed of magnetic particles. Under external stimuli, the magnetic field of the particles can change, which can be measured by the Hall sensors. For example, the soft magnetic skin in Figure 7(a) is fabricated by mixing the magnetic particles into the silicone rubber membrane, with a magnetometer under the bottom of the membrane for the detection of the changing magnetic field. Under local pressure, the magnetic particles in the corresponding positions squeeze each other, thus, the magnetic field changes. With such a simple structure, the sensor can measure continuous local deformation [14]. The magnet [11] is located right above the Hall sensor. Under normal force or shear force, the magnetic field changes when the magnet approaches or deflects the Hall sensor. So the sensor can measure the magnitude and direction of the force. Similarly, the magnetic sensor matrix [57] can be distributed on the fingertip of the robotic gripper. The sensor can map the magnetic field of each point to the 3D shape of the objects when the gripper touches them. Magnetic sensors can also be applied to measure deformation. As is shown in Ref. [58], two magnet-Hall sensor pairs are separately located at two joints of the continuum robotic arm which is actuated by SMA. When the robotic arm bends, the magnetic fields of the two pairs change. Combined with the kinematic model, the posture of the arm can be calculated with the feedback of the two sensors.

Besides the magnetic part and Hall sensor pair, there are also magnetic sensors that utilize special materials such as Giant Magneto Resistance (GMR). Under a magnetic field, the resistance of GMR decreases significantly, so GMR can be used to sense the change of the magnetic field. As the sensor in Figure 7(b) shows, it contains three layers: the hollow PDMS membrane, the magnetic membrane with the pyramid structure, and the GMR sensor. When a permanent magnet approaches the sensor, the magnetic field between the magnetic membrane and the GMR sensor decreases, so the resistance of GMR accordingly decreases. When the sensor is compressed, the distance between the magnetic membrane and the GMR decreases, and the magnetic field increases, which leads to an increase in the resistance [59]. With the reverse



changing of resistance, the sensor can clearly distinguish contact and proximity signals and accomplish tactile feedback.

3.4 Optical Waveguide Sensors

Optical waveguide sensors, which are usually composed of an emitter, a receiver, and an intermediary, can also measure force and deformation based on the change of the optical signal. The optical signal, which is generated

by the emitter, propagates to the receiver via the intermediary. When the intermediary is deformed by external forces or stretching, the refractive index or the intensity of the light changes, so the sensor can measure these signals. The optical strain sensor in Figure 8 uses the cylindrical PDMS, which is fabricated via the tubular mold, as the intermediary. Because of the high ductility of PDMS, the PDMS intermediary can be knotted or stretched. When this waveguide is stretched, the light fades because

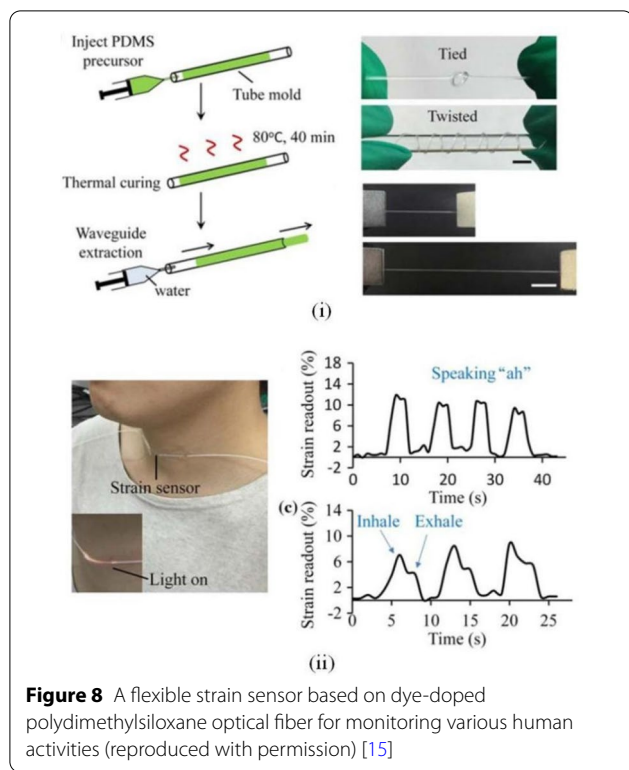


Figure 8 A flexible strain sensor based on dye-doped polydimethylsiloxane optical fiber for monitoring various human activities (reproduced with permission) [15]

of the changing of the refractive index. When attached to the human throat, the sensor can measure signals such as phonating and breathing [15]. The tactile sensor array in Ref. [60] consists of a soft bump array, an emitter, and an imaging system. When the bumps at different locations are deformed by external forces, the intensities of the light in those bumps change, thus the local forces can be mapped into a stress nephogram via the imaging system. In Ref. [61], the pressure sensor array is composed of an illumination system, force-sensing cells, and an imaging system. A force-sensing cell consists of an injection fiber,

two reception fibers, a tracer, and elastic material. Under external forces, the position of the tracer changes, and the intensity of the light in the reception fiber changes. Thus, the magnitude and direction of the force can be measured by the triangulation principle. The optical strain sensor in Ref. [62] consists of a LED, a stretchable waveguide, and a photodiode. The light is emitted from the LED, transmitted in the waveguide, and received by the photodiode. When the waveguide is stretched, the refractive index of light changes. By distributing the sensors in the upper, middle, and lower sections of the pneumatic soft finger, the deforming of the finger can be measured. Thus, the soft hand can identify the shape or the texture of the objects by touching them. The bending sensor in Ref. [63] consists of a LED, a photodiode, and a cavity enclosed by a discrete reflecting layer. Under bending, micro-cracks generate in the reflecting layer and some light loses. So, the sensor can sense the bending of the actuator.

3.5 Comparison and Potential Application in Robotics

As shown in Table 2, resistive sensors are the simplest ones to measure. Applying a constant voltage or current to the sensor, we can measure the resistance changing using a differential resistor or directly measuring the voltage. And the stretchability of the sensor is determined by the carrier, so the sensors can measure very large strain if we select a hyperelastic carrier. However, these kinds of sensors have serious hysteresis, so they are not qualified for dynamic feedback. For pressure measurements, their sensitivity is not high enough because of their finite deformation. In contrast, capacitive sensors have little hysteresis and high sensitivities for both force and strain measurement, taking advantage of their microstructured sensing layer. With complicated structures, they can measure multi-directional forces, even their directions. However, these sensors are sensitive to

Table 2 Comparison and potential application of soft sensors in robotics

Soft sensor	Resistance sensor	Capacitance sensor	Magnetic sensor	Optical waveguide sensor
Advantages	Stretchable; Larger strain; Simple structure; Low cost	High sensitivity; Low hysteresis; Fast response; Low power consumption; Simple design	Low hysteresis; Compact structure; Low cost; Contact-free sensing capability;	Inherent electrical safety; Immunity to electromagnetic interference; Small size; Low hysteresis
Limitations	High hysteresis; Nonlinear signal; Affected by the electric field, magnetic field, vibration, temperature	High cost; Affected by the external electric and magnetic field	Affected by the external electric and magnetic field	Low stretchability and stiff of traditional optical fibers
Applications	Measure tensile deformation, normal force, shear force, bending degree; Flexible touch screen; Electronic skin, etc.	Measure tensile deformation, normal force and shear force; Flexible touch screen; Electronic skin, etc.	Deformation detection; Force recognition; Shape and posture recognition	Measure force, deformation and bending; Identify shapes and textures of objects

noises that disturb the electric field, and the changing of environmental temperature and moisture. Similar to capacitive sensors, magnetic sensors are easy to be disturbed by the external magnetic field. But they can easily measure 3D forces with a simple structure since the forces will change the 3D distribution of the magnetic field. However, they are difficult to measure the strain information, and their repeatability and sensitivity need to be further investigated. Optical waveguide sensors are immune to the changing of the electric or magnetic field, so they can be used in some rigorous environments. By selecting a proper material like PDMS as the intermedia to transmit the light, they can measure the strain information. One of the disadvantages is that for the force distribution measurement, they usually need an imaging system, so it is difficult for the aim of a portable sensing system. What's more, their size is usually big, so they are difficult to be miniaturized.

For robotic applications, we must consider the parameters of the sensors (measurement range, sensitivity, and resolution, etc.), the desired information for the robots (force, direction, and deformation, etc.), and the working environments of the robots. Generally, based on the characteristics of the different kinds of sensors (Table 2), for strain measurement, the resistive sensor and stretchable optic waveguides are better choices. For measuring the magnitude and direction of forces, both capacitive sensors and magnetic sensors can be used, but safety precautions need to be considered to prevent the distribution of external electric or magnetic fields. Optical waveguide sensors can measure the force information without the affection of electric or magnetic interference, but we need to consider if the data acquisition system is acceptable.

4 Conclusions

To have a better understanding of the role of smart materials in the evolution of robotics, In this review, we present some typical smart materials for the development of soft actuators and soft sensors. For soft actuators, we mainly introduced the mechanisms and properties of electrically responsive actuators, thermally responsive actuators, magnetically responsive actuators, and photoresponsive actuators. For soft sensors, we focused on the resistive sensors, capacitive sensors, magnetic sensors, and optical waveguide sensors, and introduced their principles for measuring the deformation and force information. By comparing the advantages and disadvantages of different types of actuators and sensors, we analyzed their potential applications in robotics. Although most of the materials are still in the laboratory state, with their exploration in robotics, and more and more scientific

problems being solved, we believe they can be commercialized and to be deployed in robotic applications in the future.

Acknowledgments

Not applicable.

Author contributions

YH wrote the manuscript; SZ and BF wrote the part manuscript and edited the figures. FS and HL gave some advice on the manuscript; FS, YH and HL assisted with the structure and language of the manuscript. All authors read and approved the final manuscript.

Authors' information

Yufei Hao, born in 1990, is currently an associate professor at *School of Mechanical Engineering, University of Science and Technology Beijing, China*. He received his Ph.D. degree from *Beihang University, China*, in 2020. He has been a Postdoc fellow at *Soft Transducers Laboratory (LMTS), Ecole Polytechnique Fédérale de Lausanne (EPFL), Switzerland*. His research interests include smart materials, robotic design, soft robotic grasping, and soft sensors. E-mail: yufeihao@ustb.edu.cn

Shixin Zhang, born in 1994, is currently a Ph.D. candidate in mechanical engineering at *School of Engineering and Technology, China University of Geosciences (Beijing)*. He received his master's degree from *Anhui University of Technology, China*, in 2020. His research interests include soft robotics and robot visual-tactile perception. E-mail: zhangshixin@email.cugb.edu.cn

Bin Fang, born in 1984, is currently an assistant researcher at *Department of Computer Science and Technology, Tsinghua University, China*. He received the Ph.D. degree from *Beihang University, China*, in 2014. His research interests include sensor fusion, soft robotics, and human-robot interaction. E-mail: fangbin@tsinghua.edu.cn

Fuchun Sun, born in 1964, is currently a full professor at *Department of Computer Science and Technology, Tsinghua University, China*. He received his Ph.D. degree from *Tsinghua University, China*, in 1997. His current research interest includes robotic perception and cognition. E-mail: fcsun@tsinghua.edu.cn

Huaping Liu, born in 1976, is an associate professor at *Department of Computer Science and Technology, Tsinghua University, China*. His current research interests include robotic perception and learning. He serves as an Associate Editor of some journals including the *Cognitive Computation, Neurocomputing*, the *IEEE Transactions on Industrial Informatics, IEEE Transactions on Automation Science and Engineering*, and some conferences including ICRA and IROS.

Haiyuan Li, born in 1986, currently with *School of Automation, Beijing University of Posts and Telecommunications, China*. He received the B.S. degree from *Shandong University, China*, in 2009, and the M.S. and Ph.D. degrees from *Beihang University, China*, in 2012 and 2016, respectively. He has been a Visiting PhD at *Whiting School of Engineering, Johns Hopkins University, USA*, from 2014 to 2015. His current research interests include medical robotics, robot hand and exoskeleton, self-assembly/self-reconfigurable swarm robots.

Funding

Supported by National Key Research and Development Program of China (Grant No. 2019YFB 1309800), National Natural Science Foundation of China (Grant Nos. 62173197, 91848206), and Beijing Science & Technology Project (Grant No. Z191100008019 008).

Competing interests

The authors declare no competing financial interests.

Author Details

¹School of mechanical engineering, University of Science and Technology Beijing, Beijing 100083, China. ²School of Engineering and Technology, China University of Geosciences (Beijing), Beijing 100083, China. ³Department of Computer Science and Technology, Tsinghua National Laboratory for Information Science and Technology, Tsinghua University, Beijing 100084, China. ⁴School of Automation, Beijing University of Posts and Telecommunications, Beijing 100876, China.

Received: 7 September 2020 Revised: 24 November 2021 Accepted: 24 February 2022
Published online: 09 April 2022

References

- [1] Z Chen, F Gao, Y Pan, et al. Novel door-opening method for six-legged robots based on only force sensing. *Chinese Journal of Mechanical Engineering*, 2017, 30(5): 1227–1238.
- [2] J Carpentier, N Mansard. Multicontact locomotion of legged robots. *IEEE Transactions on Robotics*, 2018, 34(6): 1441–1460.
- [3] C Wang, K Sim, J Chen, et al. Soft ultrathin electronics innervated adaptive fully soft robots. *Advanced Materials*, 2018, 30(13): 1706695.1–1706695.9.
- [4] Y Tang, L Qin, X Li, et al. A frog-inspired swimming robot based on dielectric elastomer actuators. *IEEE/RSJ International Conference on Intelligent Robots & Systems*, Vancouver, BC, Canada, September 24–28, 2017: 2403–2408.
- [5] S Seok, C D Onal, K J Cho, et al. Meshworm: A peristaltic soft robot with antagonistic nickel titanium coil actuators. *IEEE-ASME Transactions on Mechatronics*, 2013, 18(5): 1485–1497.
- [6] Z Ren, W Hu, X Dong, et al. Multi-functional soft-bodied jellyfish-like swimming. *Nature Communications*, 2019, 10(1): 1–2.
- [7] M P Cunha, S Ambergen, M G Debije, et al. A soft transporter robot fueled by light. *Advanced Science*, 2020, 7(5): 1902842.
- [8] S Shian, K Bertoldi, D R Clarke. Dielectric elastomer based “grippers” for soft robotics. *Advanced Materials*, 2015, 27(43): 6814–6819.
- [9] B Mazzolai, L Margheri, M Cianchetti, et al. Soft-robotic arm inspired by the octopus: II. From artificial requirements to innovative technological solutions. *Bioinspiration & Biomimetics*, 2012, 7(2): 025005.
- [10] Q Shen, T Wang, J Liang, et al. Hydrodynamic performance of a biomimetic robotic swimmer actuated by ionic polymer-metal composite. *Smart Materials and Structures*, 2013, 22(7).
- [11] T Paulino, P Ribeiro, M Neto, et al. Low-cost 3-axis soft tactile sensors for the human-friendly robot Vizzy. *International Conference on Robotics and Automation*, Singapore, May 29–June 3, 2017: 966–971.
- [12] Y L Park, B R Chen, R J Wood. Soft artificial skin with multi-modal sensing capability using embedded liquid conductors. *IEEE Sensors*, Limerick, Ireland, October 28–31, 2011: 81–84.
- [13] A Atalay, V Sanchez, O Atalay, et al. Batch fabrication of customizable silicone-textile composite capacitive strain sensors for human motion tracking. *Advanced Materials Technologies*, 2017, 2(9): 1700136.
- [14] T Hellebrekers, O Kroemer, C Majidi. Soft magnetic skin for continuous deformation sensing. *Advanced Intelligent Systems*, 2019, 1(4).
- [15] J Guo, M Niu, C Yang. Highly flexible and stretchable optical strain sensing for human motion detection. *Optica*, 2017, 4(10): 1285.
- [16] C Cao, X Gao, A T Conn. A magnetically coupled dielectric elastomer pump for soft robotics. *Advanced Materials Technologies*, 2019, 4(8).
- [17] J Shintake, V Cacucciolo, H Shea, et al. Soft biomimetic fish robot made of dielectric elastomer actuators. *Soft Robotics*, 2018, 5(4): 466–474.
- [18] X Ji, X Liu, V Cacucciolo, et al. An autonomous untethered fast soft robotic insect driven by low-voltage dielectric elastomer actuators. *Science Robotics*, 2019, 4(37).
- [19] J Shintake, S Rosset, B Schubert, et al. Versatile soft grippers with intrinsic electroadhesion based on multifunctional polymer actuators. *Advanced Materials*, 2016, 28(2): 231–238.
- [20] G Gu, J Zou, R Zhao, et al. Soft wall-climbing robots. *Science Robotics*, 2018, 3(25).
- [21] E Acome, S K Mitchell, T G Morrissey, et al. Hydraulically amplified self-healing electrostatic actuators with muscle-like performance. *Science*, 2018, 359(6371): 61–65.
- [22] S K Mitchell, X Wang, E Acome, et al. An easy-to-implement toolkit to create versatile and high performance HASEL actuators for Untethered Soft Robots. *Advanced Science*, 2019, 6(14): 1900178.
- [23] Y Li, M Guo, Y Li. Recent advances in plasticized PVC gels for soft actuators and devices: A review. *Journal of Materials Chemistry C*, 2019, 7(42): 12991–13009.
- [24] X Cheng, W Yang, L Cheng, et al. Tunable-focus negative poly (vinyl chloride) gel microlens driven by unilateral electrodes. *Journal of Applied Polymer Science*, 2018, 135(15): 46136.
- [25] A Zatopa, S Walker, Y Menguc. Fully soft 3D-printed electroactive fluidic valve for soft hydraulic robots. *Soft Robotics*, 2018, 5(3): 258–271.
- [26] Y Hao, Z Liu, J Liu, et al. A soft gripper with programmable effective length, tactile and curvature sensory feedback. *Smart Materials and Structures*, 2020, 29(3): 035006.
- [27] S Felton, M Tolley, E Demaine, et al. A method for building self-folding machines. *Science*, 2014, 345(6197): 644–646.
- [28] T Chen, K Shea. An autonomous programmable actuator and shape reconfigurable structures using bistability and shape memory polymers. *3D Printing and Additive Manufacturing*, 2018, 5(2).
- [29] A M Hubbard, E Luong, A Ratanaphruks, et al. Shrink films get a grip. *ACS Applied Polymer Materials*, 2019.
- [30] R Mikołaj, Z Hao, X Chen, et al. Light-driven soft robot mimics caterpillar locomotion in natural scale. *Advanced Optical Materials*, 2016, 4(11): 1689–1694.
- [31] A Byoungkwon, S Miyashita, A Ong, et al. An end-to-end approach to self-folding origami structures by uniform heat. *IEEE Transactions on Robotics*, 2017, 34(6).
- [32] H T Lin, G G Leisk, B Trimmer. GoQBot: a caterpillar-inspired soft-bodied rolling robot. *Bioinspiration & Biomimetics*, 2011, 6(2): 026007.
- [33] W Hu, G Z Lum, M Mastrangeli, et al. Small-scale soft-bodied robot with multimodal locomotion. *Nature*, 2018, 554(7690): 81–85.
- [34] Y Kim, H Yuk, R Zhao, et al. Printing ferromagnetic domains for untethered fast-transforming soft materials. *Nature*, 2018, 558(7709): 274–279.
- [35] Y Kim, G A Parada, S Liu, et al. Ferromagnetic soft continuum robots. *Science Robotics*, 2019, 4(33): eaax7329.
- [36] G Mao, M Drack, M Karami-Mosammam, et al. Soft electromagnetic actuators. *Science Advances*, 2020, 6(26): eabc0251.
- [37] R Dong, Y Hu, Y Wu, et al. Visible-light-driven BiOI-based Janus micromotor in pure water. *Journal of the American Chemical Society*, 2017, 139(5): 1722–1725.
- [38] O M Wani, R Verpaalen, H Zeng, et al. An artificial nocturnal flower via humidity-gated photoactuation in liquid crystal networks. *Advanced Materials*, 2019, 31(2): 1805985.
- [39] H Yang, W R Leow, T Wang, et al. 3D printed photoresponsive devices based on shape memory composites. *Advanced Materials*, 2017, 29(33): 1701627.1–1701627.7.
- [40] D Vogt, Y L Park, R J Wood. A soft multi-axis force sensor. *IEEE Sensors*, Taipei, Taiwan, China, October 28–31, 2012: 1–4.
- [41] X Shi, C H Cheng, Y Zheng, et al. An EGaIn-based flexible piezoresistive shear and normal force sensor with hysteresis analysis in normal force direction. *Journal of Micromechanics and Microengineering*, 2016, 26(10): 105020.
- [42] G Gu, H Xu, S Peng, et al. Integrated soft ionotropic skin with stretchable and transparent hydrogel-elastomer ionic sensors for hand-motion monitoring. *Soft Robotics*, 2019, 6(3): 368–76.
- [43] C F Hu, W S Su, W Fang. Development of patterned carbon nanotubes on a 3D polymer substrate for the flexible tactile sensor application. *Journal of Micromechanics & Microengineering*, 2011, 21(11): 115012.
- [44] R L Truby, M Wehner, A K Grosskopf, et al. Soft somatosensitive actuators via embedded 3D printing. *Advanced Materials*, 2018, 30(15): 1706383.1–1706383.8.
- [45] R L Truby, C D Santina, D Rus. Distributed proprioception of 3D configuration in soft, sensorized robots via deep learning. *IEEE Robotics and Automation Letters*, 2020, 5(2): 3299–3306.
- [46] C Mu, Y Song, W Huang, et al. Flexible normal-tangential force sensor with opposite resistance responding for highly sensitive artificial skin. *Advanced Functional Materials*, 2018, 28(18): 1707503.
- [47] C Pang, G Y Lee, T I Kim, et al. A flexible and highly sensitive strain-gauge sensor using reversible interlocking of nanofibres. *Nature Materials*, 2012, 11(9): 795–801.
- [48] S H Cho, S W Lee, S Yu, et al. Micropatterned pyramidal ionic gels for sensing broad-range pressures with high sensitivity. *ACS Applied Materials & Interfaces*, 2017, 9(11): 10128–10135.
- [49] S Kang, J Lee, S Lee, et al. Highly sensitive pressure sensor based on bio-inspired porous structure for real-time tactile sensing. *Advanced Electronic Materials*, 2016, 2(12): 1600356.
- [50] D Kwon, T I Lee, J Shim, et al. Highly sensitive, flexible and wearable pressure sensor based on a giant piezocapacitive effect of three-dimensional microporous elastomeric dielectric layer. *ACS Applied Materials & Interfaces*, 2016, 8(26): 16922–16931.

- [51] S Peng, S Chen, Y Huang, et al. High sensitivity capacitive pressure sensor with bi-layer porous structure elastomeric dielectric formed by a facile solution based process. *IEEE Sensors*, 2018, 3(2): 1–4.
- [52] L Ma, X Shuai, Y Hu, et al. A highly sensitive and flexible capacitive pressure sensor based on a micro-arrayed polydimethylsiloxane dielectric layer. *Journal of Materials Chemistry C*, 2018, 6(48): 13232–13240.
- [53] P Roberts, D D Damian, W Shan, et al. Soft-matter capacitive sensor for measuring shear and pressure deformation. *International Conference on Robotics and Automation*, Karlsruhe, Germany, May 6–10, 2013: 3529–3534.
- [54] L Viry, A Levi, M Totaro, et al. Flexible three-axial force sensor for soft and highly sensitive artificial touch. *Advanced Materials*, 2014, 26(17): 2659–2664.
- [55] Y Huang, H Yuan, W Kan, et al. A flexible three-axial capacitive tactile sensor with multilayered dielectric for artificial skin applications. *Microsystem Technologies*, 2017, 23(6): 1847–1852.
- [56] C M Boutry, M Negre, M Jorda, et al. A hierarchically patterned, bio-inspired e-skin able to detect the direction of applied pressure for robotics. *Science Robotics*, 2018, 3(24): eaau6914.
- [57] T P Tomo, A Schmitz, W K Wong, et al. Covering a robot fingertip with uSkin: A soft electronic skin with distributed 3-axis force sensitive elements for robot hands. *International Conference on Robotics and Automation*, Brisbane, Australia, May 21–25, 2018, 3(1): 124–131.
- [58] H Guo, F Ju, Y Cao, et al. Continuum robot shape estimation using permanent magnets and magnetic sensors. *Sensors and Actuators A: Physical*, 2019, 285: 519–530.
- [59] J Ge, X Wang, M Drack, et al. A bimodal soft electronic skin for tactile and touchless interaction in real time. *Nature Communications*, 2019, 10(1): 1–10.
- [60] H Liu, J Back, K Althoefer. Feasibility study-novel optical soft tactile array sensing for minimally invasive surgery. *IEEE/RSJ International Conference on Intelligent Robots & Systems*, Hamburg, Germany, September 28–October 02, 2015: 1528–1533.
- [61] Llamosiartemis, Toussaintseverine. Measuring force intensity and direction with a spatially resolved soft sensor for biomechanics and robotic haptic capability. *Soft Robotics*, 2019, 6(3): 346–355.
- [62] H Zhao, O Brien, Kevin, S Li, et al. Optoelectronically innervated soft prosthetic hand via stretchable optical waveguides. *Science Robotics*, 2016, 1(1): eaai7529.
- [63] J Jung, M Park, D Kim, et al. Optically sensorized elastomer air chamber for proprioceptive sensing of soft pneumatic actuators. *International Conference on Robotics and Automation*, Paris, France, May 31–Jun 4, 2020, 5(2): 2333–2340.

Submit your manuscript to a SpringerOpen[®] journal and benefit from:

- Convenient online submission
- Rigorous peer review
- Open access: articles freely available online
- High visibility within the field
- Retaining the copyright to your article

Submit your next manuscript at ► [springeropen.com](https://www.springeropen.com)
